Journal of Hepatocellular Carcinoma

Dovepress
open access to scientific and medical research

Open Access Full Text Article

ORIGINAL RESEARCH

Plumbagin Regulates Snail to Inhibit Hepatocellular Carcinoma Epithelial-Mesenchymal Transition in vivo and in vitro

Yuan-Qin Du[1,*], Bin Yuan[1,*], Yi-Xian Ye[1], Feng-ling Zhou[1], Hong Liu[1], Jing-Jing Huang[2], Yan-Fei Wei[3,4]

[1]Graduate School, Guangxi University of Traditional Chinese Medicine, Nanning, 530200, People's Republic of China; [2]The First Affiliated Hospital of Guangxi University of Chinese Medicine, Nanning, 530024, People's Republic of China; [3]Department of Physiology, Guangxi University of Traditional Chinese Medicine, Nanning, 530200, People's Republic of China; [4]Guangxi Key Laboratory of Translational Medicine for Treating High-Incidence Infectious Diseases with Integrative Medicine, Nanning, 530200, People's Republic of China

*These authors contributed equally to this work

Correspondence: Yan-Fei Wei, Department of Physiology, Guangxi University of Traditional Chinese Medicine, No. 13 Wu He Road, Nanning, 530200, People's Republic of China, Tel/Fax +86-771-4733794, Email weiyanfei@gxtcmu.edu.cn

Background/Aims: Plumbagin (PL) has been shown to effe ctively inhibit autophagy, suppressing invasion and migration of hepatocellular carcinoma (HCC) cells. However, the specific mechanism remains unclear. This study aimed to investigate the effect of PL on tumor growth factor (TGF)-β-induced epithelial-mesenchymal transition (EMT) in HCC.

Methods: Huh-7 cells were cultured, and in vivo models of EMT and HCC-associated lung metastasis were developed through tail vein and in situ injections of tumor cells. In vivo imaging and hematoxylin and eosin staining were used to evaluate HCC modeling and lung metastasis. After PL intervention, the expression levels of Snail, vimentin, E-cadherin, and N-cadherin in the liver were evaluated through immunohistochemistry and Western blot. An in vitro TGF-β-induced cell EMT model was used to detect Snail, vimentin, E-cadherin, and N-cadherin mRNA levels through a polymerase chain reaction. Their protein levels were detected by immunofluorescence staining and Western blot.

Results: In vivo experiments demonstrated that PL significantly reduced the expression of Snail, vimentin, and N-cadherin, while increasing the expression of E-cadherin at the protein levels, effectively inhibiting HCC and lung metastasis. In vitro experiments confirmed that PL up-regulated epithelial cell markers, down-regulated mesenchymal cell markers, and inhibited EMT levels in HCC cells.

Conclusion: PL inhibits Snail expression, up-regulates E-cadherin expression, and down-regulates N-cadherin and vimentin expression, preventing EMT in HCC cells and reducing lung metastasis.

Keywords: plumbagin, hepatocellular carcinoma, epithelial-mesenchymal transition, pulmonary metastasis, Snail

Introduction

Hepatocellular carcinoma (HCC) is the most common type of liver cancer, accounting for approximately 75–85% of primary liver cancer cases.[1] It ranks as the sixth most prevalent malignant tumor globally[2] and has become the second leading cause of cancer-related deaths.[3] The low survival rate of HCC results from it being asymptomatic in the early stage. Timely diagnosis in the mid to late stages allows for extended survival through interventions like arterial chemoembolization and chemoradiotherapy. Delayed diagnosis often leads to metastasis, significantly impacting the efficacy of local or systemic treatment.[4] Lung metastasis accounts for 38.4–53.8% of extrahepatic metastases, being the most common type of extrahepatic metastasis of liver cancer. The one-year survival rate of patients with lung metastasis is approximately 10%.[5]

Understanding the mechanisms underlying liver cancer recurrence and metastasis by focusing on epithelial-mesenchymal transformation (EMT), a phenomenon crucial for tumor development, invasion, and metastasis, is vital for improving overall treatment outcomes for patients with HCC.[6] EMT, a biological process, involves the morphological

Received: 20 December 2023
Accepted: 1 March 2024
Published: 19 March 2024

transformation of epithelial cells into mesenchymal cells, resulting in loss of cell polarity, cytoskeletal rearrangement, and increased mobility.[7] Key manifestations include the down-regulation of epithelial cell markers such as E-cadherin and β-catenin, and the up-regulation of mesenchymal cell markers such as N-cadherin and vimentin.[8]

Tumor growth factor (TGF)-β/suppressor of mothers against decapentaplegic (Smad), Notch, and Wingless-related integration site (Wnt)/β-catenin are the main signaling pathways involved in EMT. Additionally, different signaling transduction pathways regulate the expression of EMT-related genes by activating small molecular weight transcription factors, known as EMT-induced transcription factors (EMT-TF), including Snail-1/2, Twist-1/2, and (Zinc finger E-box-binding protein 1/2) ZEB-1/2, which serve as markers for mesenchymal cells.[9]

Mounting evidence indicates EMT activation in HCC occurrence, growth, progression, metastasis, and drug resistance.[10,11] The tumor microenvironment, characterized by hypoxia and heightened inflammation, stimulates the acquisition of migratory and invasive capabilities by HCC cells, facilitating cancer cell localization to other tissues.[12] Because EMT endows cancer cells with strong migration and invasion capabilities, it plays a crucial role in early liver cancer metastasis and recurrence.[13] Furthermore, cancer cells undergoing EMT exhibit reduced sensitivity to various anti-cancer treatments and drug resistance.[14,15] Inhibiting EMT in patients with HCC can reduce the resistance of sorafenib.[16] Thus, current research focuses on developing therapeutic strategies and drugs for HCC by targeting the inhibition of EMT in HCC cells. For example, at present, HCC patients who failed sorafenib treatment can continue to be treated with (tumor microenvironment) TME related therapies. Immunotherapy represented by immune checkpoint inhibitors (ICIS) and targeted therapy represented by tyrosine kinase inhibitors (TKIs) can greatly improve the prognosis of HCC by inhibiting EMT.[17]

Due to severe side effects associated with conventional and synthetic drugs used in the treatment of HCC, an alternative treatment might offer a safer and more effective approach. Certain Chinese medicines and compounds exhibit characteristics such as multi-component and multi-target capabilities,[18] by regulating various signaling pathways and subsequently inhibiting the invasion and metastasis of liver cancer cells.[19] Therefore, identifying traditional and herbal medicines with potential therapeutic effects on liver cancer is essential.

Plumbagin (PL), a natural naphthoquinone compound primarily derived from the root of *Plumbago zeylanica* L, possesses various pharmacological activities, including anti-cancer, anti-fibrosis, anti-coagulation, cardiotonic, and anti-microbial effects.[20,21] Furthermore, PL exhibits significant inhibitory effects on various malignancies such as lung, breast, and prostate cancers.[22–25] PL can inhibit fibroblast growth factor 2 (FGF2) - induced EMT in breast cancer cells.[26] It induces autophagy and apoptosis in liver cancer cells both in vivo and in vitro,[27,28] inhibits SMMC-7721 cell proliferation and invasion induced by stromal cell-derived factor-1(SDF-1), significantly hinders HCC angiogenesis,[29,30] and triggers reactive oxygen species-mediated oxidative stress. This leads to DNA damage and the activation of the Ataxia Telangiectasia Mutated/P53 signaling pathway, resulting in G2/M phase arrest of HCC cells.[31]

A network pharmacology study identified tumor protein P53, mitogen-activated protein kinase (MAPK)1, MAPK2, Rapidly Accelerated Fibrosarcoma 1 (RAF1), and cyclin D1 (CCND1) as the five key targets for PL's anti-liver cancer effect. The experiment confirmed a reduction in TP53 and MAPK1 expression in liver cancer cells following treatment with PL, a reduced form of PL.[32] Reducing the expression of MAPK1, RAF1, and CCND1 promoted the proliferation, invasion, and the EMT of HCC cells.[33–35] Therefore, to comprehensively understand the anti-liver cancer mechanism of PL, this study analyzed its effect on lung metastasis by developing an in vitro tumor EMT model and two in vivo liver cancer models. Our aim was to explore the inhibition of EMT in liver cancer cells as a mechanism underlying the anti-cancer effect of PL.

Materials and Methods

Reagents

PL (4 mM, dissolved in dimethyl sulfoxide) was purchased from Sigma-Aldrich Co LLC (USA). The anti-rabbit-snail antibody was purchased from ABclonal (Wuhan, China), Inc. (A5243; dilution, 1:1000). The anti-rabbit-vimentin and anti-mouse-E-cadherin-antibodies were purchased from Abcam Inc. (Ab92547 and Ab231303; dilution 1:1000; Cambridge, UK). The anti-rabbit-N-cadherin-antibody was purchased from Cell Signaling Technology Inc. (13116s;

dilution 1:1000; Beverly, USA). The anti-β-actin antibody was purchased from Boster Biological Technology Inc. (BM0627; dilution 1:500; Wuhan, China).

Cell Lines and Culture Conditions

Human HCC cell lines (Huh7) were purchased from Procell Life Science&Technology (Wuhan, China). The Dulbecco's Modified Eagle Medium with a high-glucose content required for human HCC Huh7 cell culture and the Minimum Essential Medium required for human HCC HepG2 and SK-Hep1 cell cultures were acquired from Procell Life Science&Technology. The complete culture media were supplemented with 10% fetal bovine serum (FBS, Gibco), penicillin 100 U/mL, and streptomycin 100 μg/mL. All cells were incubated at 37 °C in an incubator with 5% CO_2.

The EMT cell model was developed by treating Huh7 cells with 10 ng/mL TGF-β for 48 h. Experiments utilized Huh7 and Huh7 EMT model cells in their logarithmic growth phase.

Cell Viability Assay

Huh7 and Huh7 EMT model cells were seeded at a density of 4×10^3 cells/well in 96-well plates. After 24 h of culturing, the media was replaced, the culture was added to the EMT model group, and the mixture was incubated for 48 h; additionally, the PL groups were exposed to various concentrations of PL (2, 4, or 8 μM) for 48 h. Cell viability was assessed using a cell counting kit-8 (CCK-8) (MedChemExpress, USA). Briefly, 10 μL of CCK-8 solution was added to the cells, followed by incubation at 37 °C for 2 h. The absorbance values at 450 nanometers were measured using a microplate reader (Multiskan MK3, Thermo Fisher Scientific, USA), with each set consisting of three replicate wells.

Animal Assay

Twenty-four 5-week-old male BALB/c nude mice, weighing 18–20 g, were purchased from Hunan Lake Jingda Experimental Animal Co., LTD., and kept in the Specific Pathogen Free animal laboratory of Guangxi University of Traditional Chinese Medicine (Animal Qualification Certificate Number: SCXK [Xiang] 2019–0004). The mice were housed in an SPF environment at a temperature of 20–24 °C and relative humidity of 50–70% with a 12-h light–dark cycle and air circulation in the animal laboratory of Guangxi University of Traditional Chinese Medicine. The mice were fed for 7 days, with free access to food and water. Huh-7-LUC stably transfected cells, grown to 90% confluency in a 75 cm^3 plate, and underwent digestion and resuspension in the complete culture medium. They were intravenously injected into the tails of mice to create an in vivo metastasis model(n=12). Then the mice were divided into control group (n=6) and PL group (n=6). In the remaining 12 mice, 1×10^6 Huh7 cells suspended in 50 μL of medium were injected into the left hepatic lobe after exposing the right abdomen under sterile conditions to construct an in situ HCC model. Again, the model mice were then divided into control groups (n=6) and PL groups (n=6). On the eighth day, mice in control group were intraperitoneally injected with normal saline (0.2 mL/d), and mice in PL group were intraperitoneally injected with PL(4 mg/kg/d). After four weeks of treatment, the mice were killed, lung and liver tissues were collected, and metastatic nodules were observed using hematoxylin and eosin (H&E) staining. All experiments have been approved by the Ethics Committee of Guangxi University of Traditional Chinese Medicine (approval number: DW20230324-116). This work was performed under supervision for the declaration of Helsinki and "Guiding Opinions on the Treatment of Animals" in China.

Bioluminescence Imaging (BLI)

The onset/development of liver metastasis was monitored using BLI. At each time point, mice received an intraperitoneal injection of phosphate-buffered saline with D-luciferin (200 mg x kg^{-1}). After 20 min, mice were anesthetized with isoflurane via inhalation, and imaging was conducted using an IVIS 200 system (PerkinElmer Imaging Systems, United States). Data were processed and reconstructed on the workstation.

Immunohistochemistry (IHC) and H&E Staining

Samples underwent dehydration in gradient alcohol, fixation in neutral-buffered formalin, and paraffin embedding. Tissue sections were prepared, dewaxed, and subjected to H&E staining. For IHC staining, antigen retrieval was achieved by

pressure cooking in 0.01 M sodium citrate buffer at 100 °C for 15 minutes. Slides were treated with 3% H_2O_2 in methanol, blocked, and incubated with rabbit anti-snail (1:50), vimentin (1:100), and mouse anti-N-cadherin (1:100) and anti-E-cadherin (1:100) antibodies overnight at 4 °C. Biotinylated secondary antibodies and a streptavidin-HRP complex (Zsbio, Wuhan, China) were applied. Images were captured using an Olympus camera (Nikon Instruments, Melville). Optical density analysis was performed on the immunohistochemical images using IPP 6.0 software. Four 400-fold images were taken for each slice to evaluate optical density. The average optical density was utilized for further analysis.

Real-Time Polymerase Chain Reaction (PCR) Assay

Total RNA was extracted from Huh7 cells using TRIzol reagent (Takara, Japan) and reverse transcribed using HiScript III Reverse Transcriptase (Vazyme, Nanjing, China). Primers, designed based on Gene Bank reference gene sequence, were used for real-time PCR messenger RNA(mRNA) detection with AceQ qPCR SYBR Green Master Mix (Vazyme). The mRNA levels of E-cadherin, N-cadherin, vimentin, and Snail were evaluated, using β-actin as the internal control. Primer sequences specific to each gene are listed in Table 1.

Immunofluorescence Staining

Huh-7 cells were seeded into 12-well plates, grown on sterilized coverslips, and exposed to the indicated treatments. Subsequently, they were fixed using 4% paraformaldehyde, permeabilized with 0.5% Triton X-100 (ST795, Beyotime, China) for 20 min at 25°C, blocked with normal goat serum for 30 min, incubated with primary antibodies against N-cadherin (1:100, CST, USA) and E-cadherin (1:100, Abcam, UK) at 4 °C overnight, and subsequently, with fluorochrome-labeled anti-rabbit and anti-mouse secondary antibodies (1:100, Boster, China) for 1 h at 25°C. The coverslips were stained with 4′,6-diamidino-2-phenylindole (DAPI; 1:5000, Beyotime) and visualized using an Olympus camera (Nikon Instruments, Melville). Images were merged using Adobe Photoshop 6.0 software.

Western Blot

The expression of EMT-related proteins in Huh7 cells or tumor tissues was detected by Western blot. Protein samples were lysed with RIPA protein lysate and quantified using a Bicinchoninic Acid Protein Concentration Assay Kit (P0010, Beyotime, China). Then, the protein samples were loaded onto sodium dodecyl-sulfate polyacrylamide gel electrophoresis gels and transferred onto polyvinylidene fluoride membranes (Millipore, Billerica, MA, USA). The membranes were blocked with 5% non-fat milk for 2 h at 25°C, and further treated with the following appropriately diluted primary antibodies: anti-β-actin (1:500), anti-snail (1:1000), anti-vimentin (1:1000), anti-E-cadherin (1:1000), and anti-N-

Table 1 mRNA Gene Primer Sequences

Name	Primer	Sequence	Size
Homo β-actin	Forward	5'- AGCGAGCATCCCCCAAAGTT −3'	285 bp
	Reverse	5'- GGGCACGAAGGCTCATCATT −3'	
Homo E-cadherin	Forward	5'- CGTAGCAGTGACGAATGTGG −3'	175 bp
	Reverse	5'- CTGGGCAGTGTAGGATGTGA −3'	
Homo N-cadherin	Forward	5'- CTTGCCAGAAAACTCCAGGG −3'	213 bp
	Reverse	5'- TGTGCCCTCAAATGAAACCG −3'	
Homo vimentin	Forward	5'- TGAGTACCGGAGACAGGTGCAG −3'	119 bp
	Reverse	5'- TAGCAGCTTCAACGGCAAAGTTC-3'	
Homo Snail	Forward	5'- ATGCACATCCGAAGCCACA −3'	190 bp
	Reverse	5'- TGACATCTGAGTGGGTCTGG −3'	

cadherin (1:1000). The blots were incubated at 4 °C overnight. After washing three times with Tris-buffered saline with tween (TBST), the corresponding secondary antibody was added, and the mixture was incubated for 2 h at 25°C. After incubation with the luminescent solution from the ECL kit (Applygen, China), the film was exposed in the cassette. The protein bands were developed, and grayscale images were scanned using Band Scan software.

Statistical Analysis

Data are expressed as mean ± standard deviation (SD). Statistical analysis was performed using SPSS 22.0. One-way ANOVA was used for comparisons between groups. The differences were considered statistically significant for *P*-values < 0.05.

Results

PL Decreased Liver and Lung Metastases in the Metastatic HCC Mouse Models

The protocol of the HCC model is summarized in Figure 1A. Live imaging results illustrated in Figure 1B and C revealed strong fluorescence in the abdominal cavity and liver of mice in the control group. Conversely, the PL group displayed markedly reduced fluorescence intensity and area, with some liver tissues showing no fluorescence emission, indicating significant inhibition of tumor metastasis. In Figure 1D, noticeable white spots or ring-shaped tumor foci were evident on the liver tissue surface in the control group. Conversely, the PL group exhibited significantly fewer liver metastasis nodules than the control group. Liver H&E staining results (Figure 1E) aligned with the in vivo imaging data, showing a substantial reduction in the number of metastases and size of tumor lesions in the PL group compared to the control group. Similarly, as shown in Figure 1F, the fluorescence intensity and area of the lungs in the PL group were significantly lower than those in the control group. In Figure 1G, lung metastatic nodules were significantly less in the PL group than in the control group. Lung he staining results (Figure 1H) were consistent with the in vivo imaging data, showing a significant reduction in the number of metastases and tumor lesion size in the PL group compared with the control group. (n=4)

PL Reduces Lung Metastases in the Orthotopic HCC Mouse Model

To further explore the involvement of EMT in HCC-associated lung metastases, an in situ HCC model was developed by injecting Huh-7-LUC cells into the left lobe of the liver (Figure 2A). Overall in vivo imaging indicated larger fluorescence intensity, area, and area transferred to nearby areas in the control group compared to the PL group (Figure 2B). As shown in Figure 2C, consistent with the liver cancer transplant tumor model, the control group exhibited conspicuous white spots or ring-shaped tumor foci on liver tissue surfaces, while the PL group showed significantly fewer such spots. Liver H&E staining demonstrated a significantly higher number of metastases and tumor size in the control group than in the PL group (Figure 2D). In vivo lung imaging revealed a larger hot spot and area in the control group than in the PL group (Figure 2E). Similarly, as shown in Figure 2F, the PL group had significantly fewer white spots or ring-shaped tumor foci in the lung tissue than the control group. Lung he staining showed that the number of metastases and tumor size were significantly lower in the PL group than in the control group (Figure 2G). This again demonstrated the inhibitory effect of PL on tumor metastasis (n=5).

PL Inhibits EMT in the Orthotopic HCC Mouse Models

Snail is a key EMT inducer, primarily characterized by the down-regulation of E-cadherin and the up-regulation of N-cadherin, vimentin, and other markers.[36] The expression of EMT-related proteins in in situ HCC liver tissue was evaluated using IHC and Western Blot. IHC revealed significantly higher expression levels of Snail, N-cadherin, and vimentin and substantially lower E-cadherin expression levels in the control group compared to the PL group (Figures 3A and B). Western blot results demonstrated a significant decrease in N-cadherin, vimentin, and Snail levels of expression in liver tissue after PL intervention, accompanied by a significant increase in E-cadherin levels (Figure 3C and D), consistent with immunohistochemical findings. These results indicated that PL down-regulates the expression of the transcriptional regulatory factor Snail, leading to the up-regulation of E-cadherin in epithelial cells and down-regulation of N-cadherin and vimentin in interstitial cells, thereby inhibiting EMT in the in situ HCC model. (n=3)

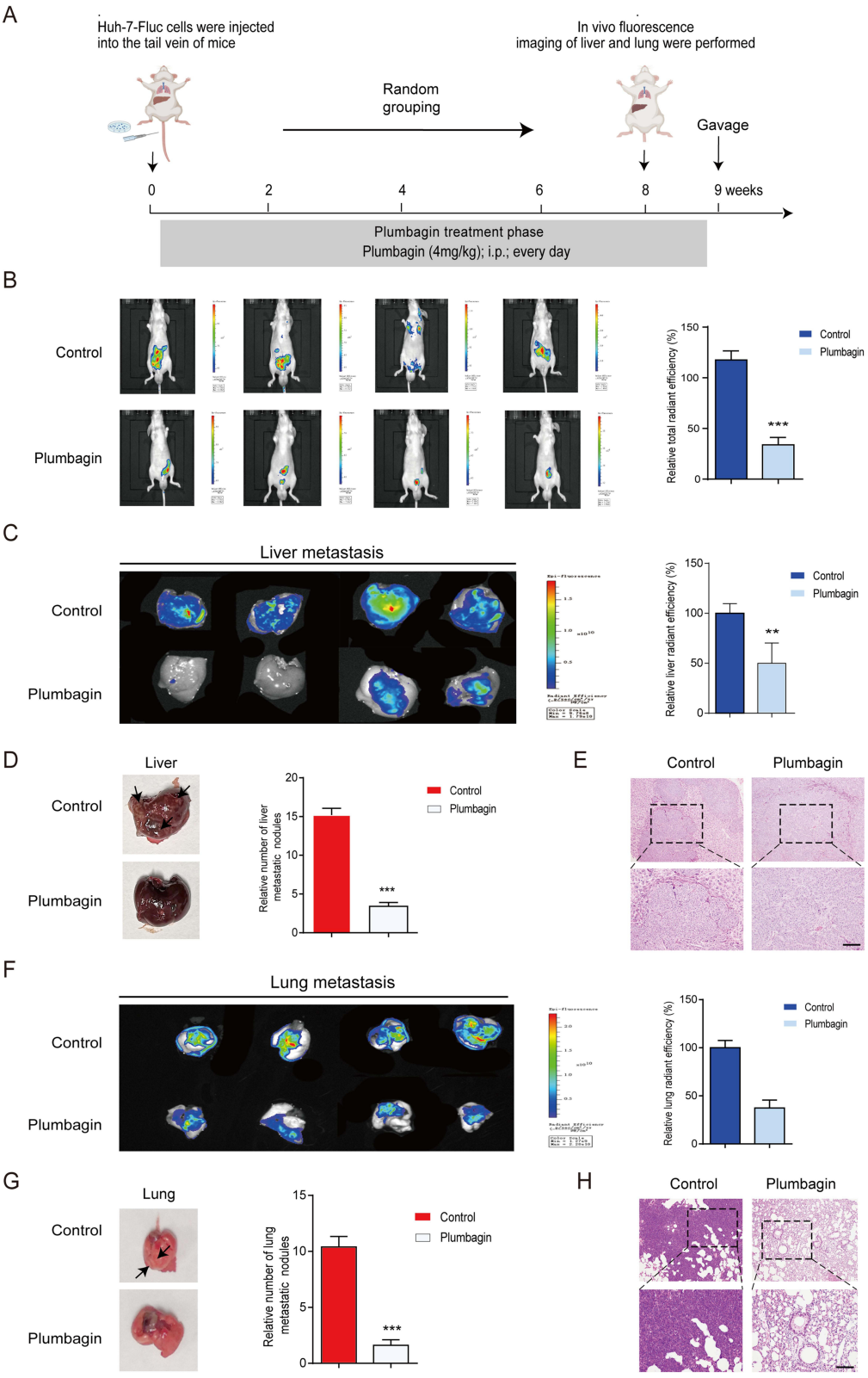

Figure 1 (**A**) Schematics of liver cancer metastasis mouse model. (**B**) Fluorescence imaging of experimental groups and fluorescence intensity comparison. (**C**) Liver fluorescence imaging for experimental groups and fluorescence intensity comparison. (**D**) Liver imaging and quantification of liver nodules in situ. (**E**) Liver hematoxylin and eosin (H&E) staining. (**F**) Lung fluorescence imaging and fluorescence intensity comparison. (**G**) Lung imaging and quantification of pulmonary nodules. (**H**) Lung H&E staining. $^{**}P < 0.01$, $^{***}P < 0.001$ vs the control group.

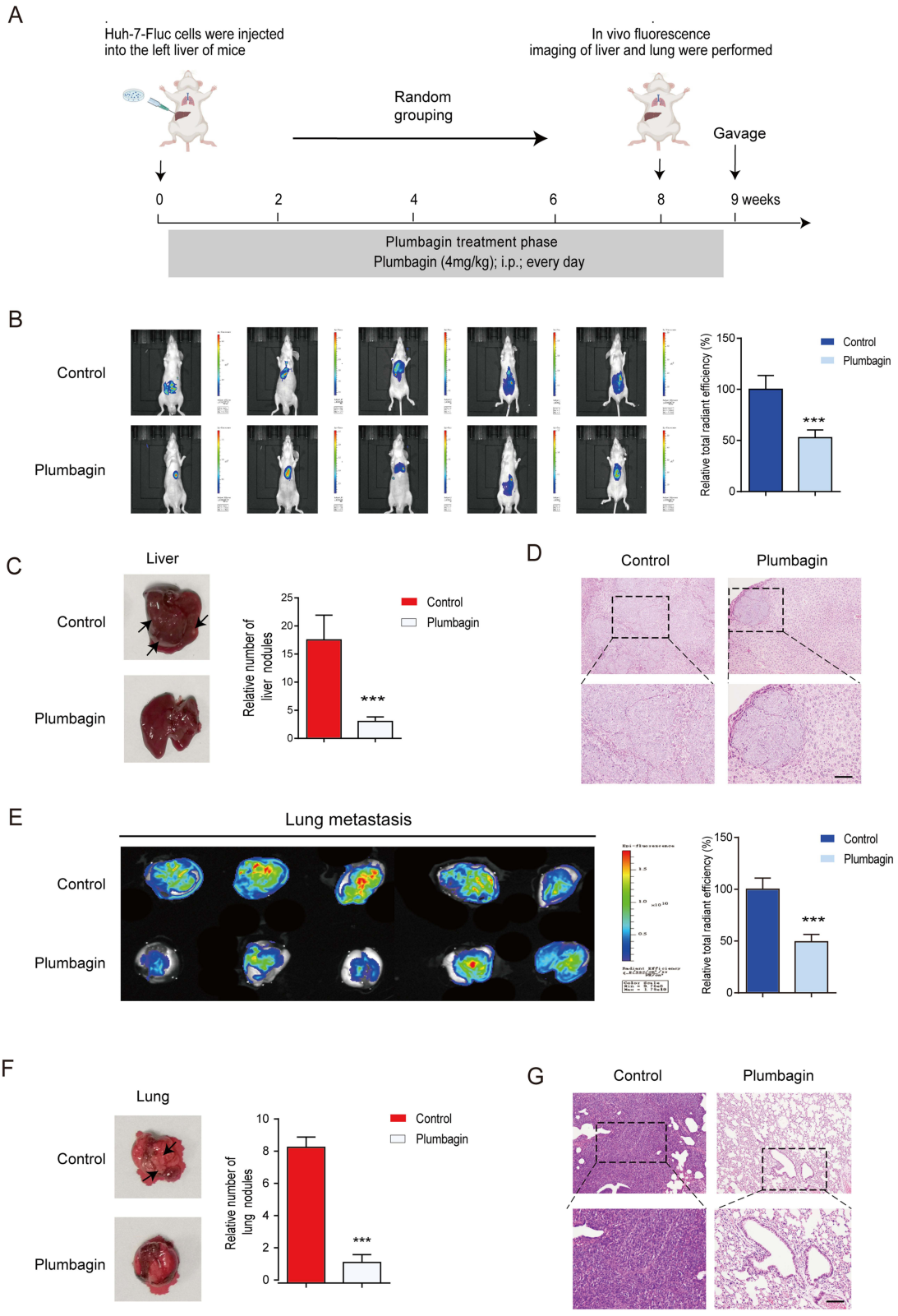

Figure 2 (**A**) Schematics of in situ liver cancer model development (**B**) Fluorescence imaging of experimental mice and comparison of fluorescence intensity. (**C**) Liver imaging and quantification of in situ liver nodules. (**D**) Liver hematoxylin and eosin (H&E) staining. (**E**) Lung fluorescence imaging and fluorescence intensity comparison. (**F**) Lung imaging and quantification of lung nodules. (**G**) Lung H&E staining. ***$P < 0.001$ vs the control group.

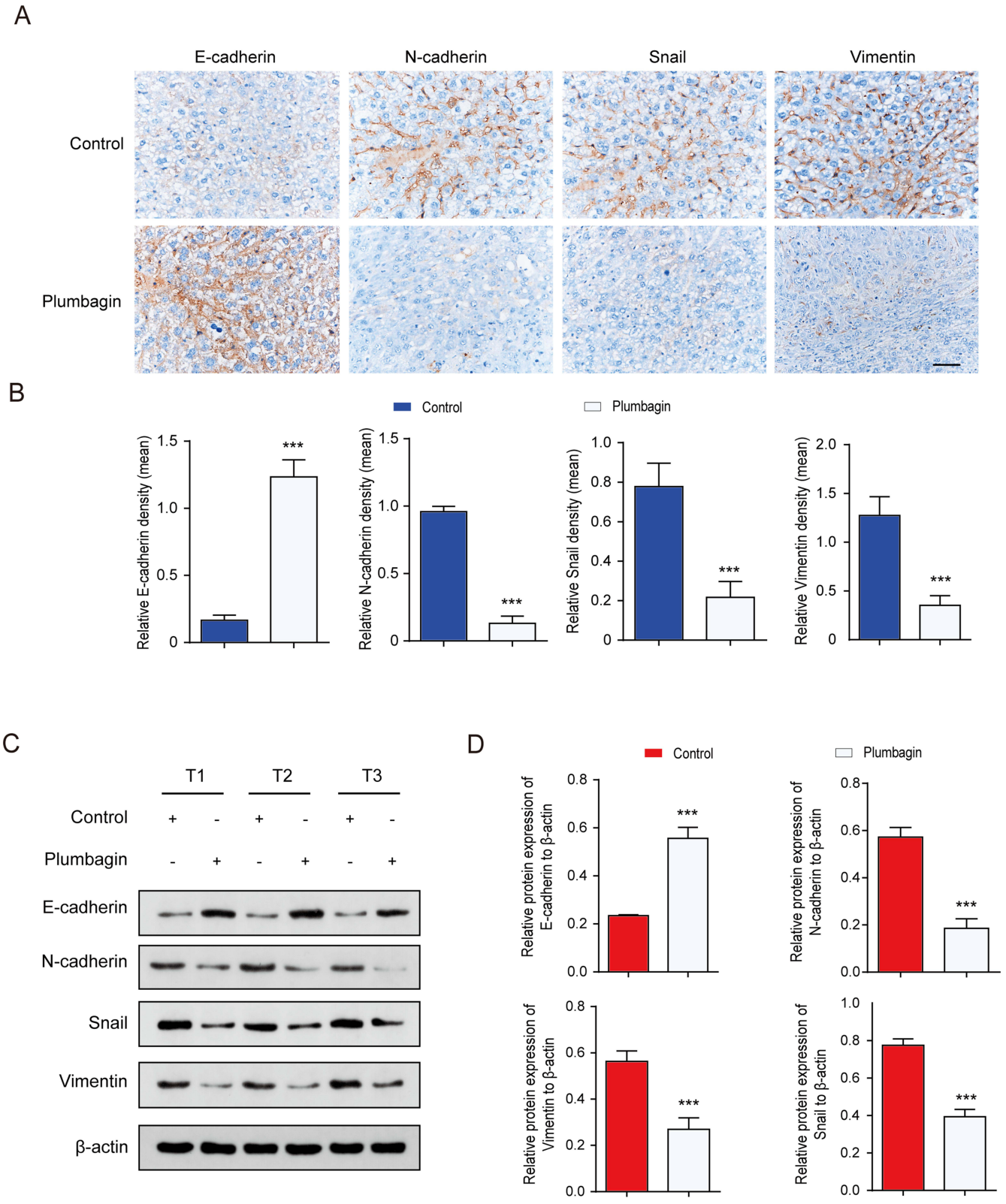

Figure 3 (**A**) Immunohistochemical (IHC) staining of liver tissue. (**B**) Quantitative expression of EMT-related proteins in liver tissue assessed using IHC. (**C**) Western blot detection of EMT-related protein bands in liver tissue. (**D**) Quantitative expression of EMT-related proteins in liver tissue. ***$p < 0.001$ vs the control group.

Development and Validation of the EMT Huh-7 Cell Model

TGF-β is a potent inducer of cellular EMT.[37] Therefore, we used it to develop an EMT cell model. The expression levels of Snail, E-cadherin, N-cadherin, and vimentin were assessed using immunofluorescence, validating the successful development of the EMT model. As illustrated in Figure 4A–D, compared to the control group, TGF-β-treated Huh-7 cells exhibited a decrease in the expression level of E-cadherin, and an increase in the expression levels of Snail, N-cadherin, and vimentin. (n=3)

The Effect of PL on TGF-β-Induced EMT in Huh-7 Cells

As illustrated in Figure 4A–D, immunofluorescence revealed differential expression patterns, with Snail being expressed in the nucleus, vimentin in the cytoplasm, and E-cadherin and N-cadherin in the cytoplasmic membrane. N-cadherin and Snail were nearly absent in normal cells but were highly expressed in the EMT model group. Vimentin exhibited a low expression in normal cells and a high expression in the EMT model group. Conversely, E-cadherin was highly expressed in normal cells and significantly decreased in the EMT model group. PL significantly increased the expression of E-cadherin and decreased that of Snail, N-cadherin, and vimentin compared to the EMT model group. These results indicated that PL significantly inhibited EMT, in a dose-dependent manner. The most pronounced inhibitory effect was observed at the concentration of 8 μM. (n=3)

PL Regulated the mRNA of EMT-Related Markers

As illustrated in Figure 5A, compared to control, the mRNA levels of N-cadherin, vimentin, and Snail significantly increased when EMT occurred, while the mRNA levels of E-cadherin significantly decreased. After PL intervention, the mRNA levels of N-cadherin, vimentin, and Snail decreased significantly, while that of E-cadherin increased. The effect was more pronounced with the increase in PL concentration. (n=3)

PL Regulates EMT-Related Signature Proteins

According to variance analysis (Figure 5B and C), the expression levels of N-cadherin, vimentin, and Snail significantly increased in the model group compared to the blank control group, while those of E-cadherin significantly decreased. The expression levels of N-cadherin, vimentin, and Snail decreased significantly in the PL group compared to the model group, while that of E-cadherin increased, with the effect being more significant with the increase in PL concentration. The results were consistent with those of qPCR, indicating that PL can effectively inhibit the EMT of HCC cells, the therapeutic effect being concentration-dependent. (n=3)

Discussion

HCC, a common and highly lethal cancer,[38] poses a significant challenge due to the limited efficacy of current surgical and chemotherapy interventions. Despite therapeutic advancements, the 5-year survival rate remains low, primarily due to adverse reactions from chemotherapy, including cachexia and drug resistance, and the inability to control tumor cell invasion and metastasis.[39] Approximately 90% of HCC-related deaths result from metastasis.[40] Effective treatment strategies must target fundamental factors involved in carcinogenesis, including metastasis. Metastasis is one of the most important mechanisms driving HCC progression. Subsequently, inhibiting metastasis is crucial for improving patient survival rates. EMT plays a key role in the early stages of metastasis.[41]

Current HCC treatment approaches both conventional and traditional, exhibit limited effectiveness, necessitating the exploration of novel treatment modalities. For example, metronomic capecitabine was well tolerated in hepatocellular carcinoma patients who had been treated with sorafenib.[42] Similarly, TME related therapies are increasingly recognized as effective treatments, and molecular targeted therapy, immunotherapy and their combination are the main approaches.[17] In recent years, the emergency of ICI and TKI has revolutionized the management of HCC.[43] Although the pioneering regimen of atezolizumab / bevacizumab is consolidating its position as the first-line treatment of advanced HCC and has made major breakthroughs in systemic treatment, HCC still predicts a poor prognosis due to drug resistance and frequent recurrence.[44] So, Identifying potential therapeutic markers and bioactive ingredients is crucial for effectively reducing

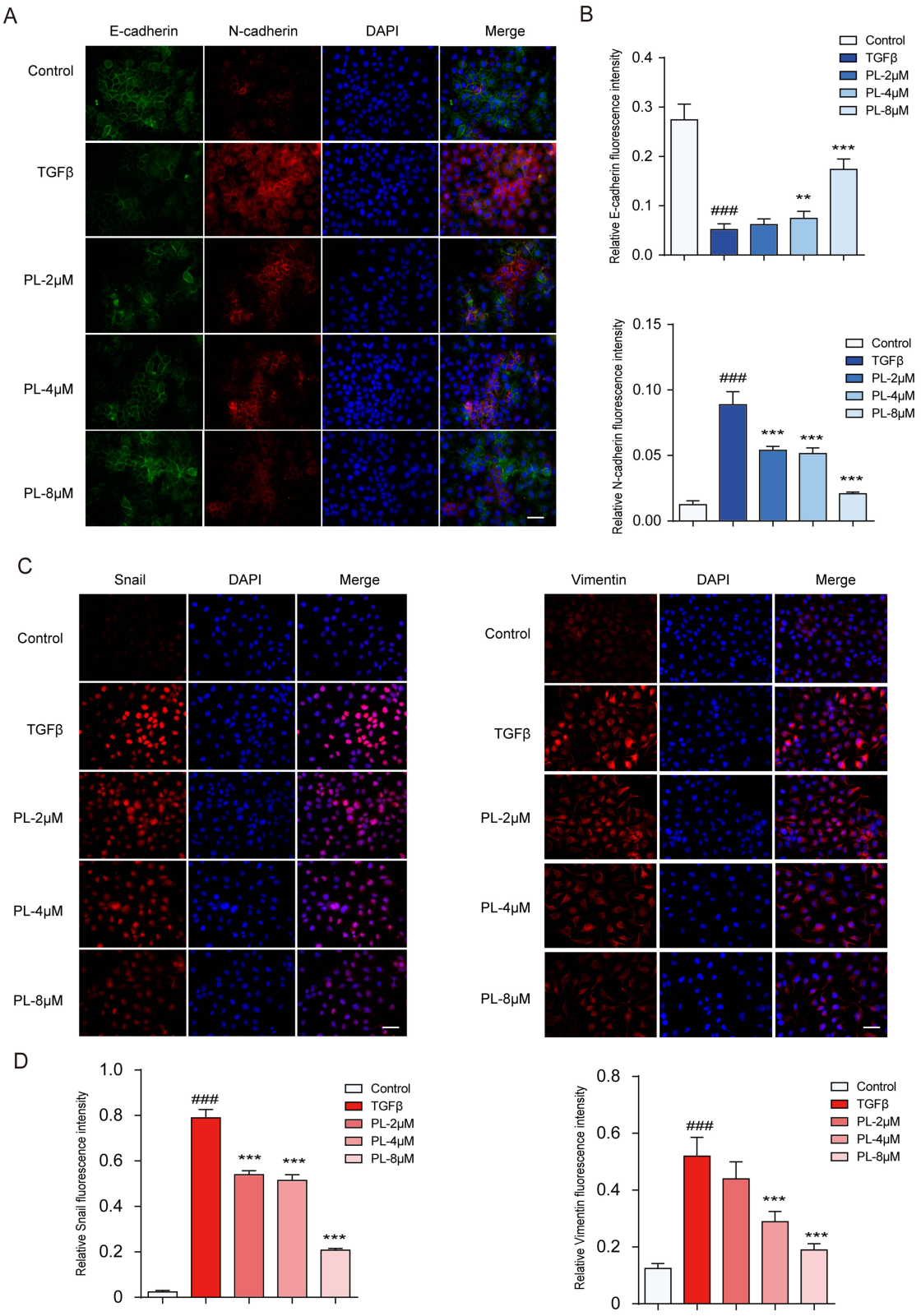

Figure 4 (**A**) The expression of E-cadherin and N-cadherin in cells determined by immunofluorescence staining. (**B**) Quantitative protein expression of E-cadherin and N-cadherin (**C**) Changes in Snail and vimentin cell expression levels measured by fluorescence staining. (**D**) Quantitative expression of Snail and vimentin proteins. In the image, DAPI stains the nucleus (blue). $^{**}P < 0.01$, $^{***}P < 0.001$ vs tumor growth factor-β group; $^{\#\#\#}P < 0.001$ vs blank group.

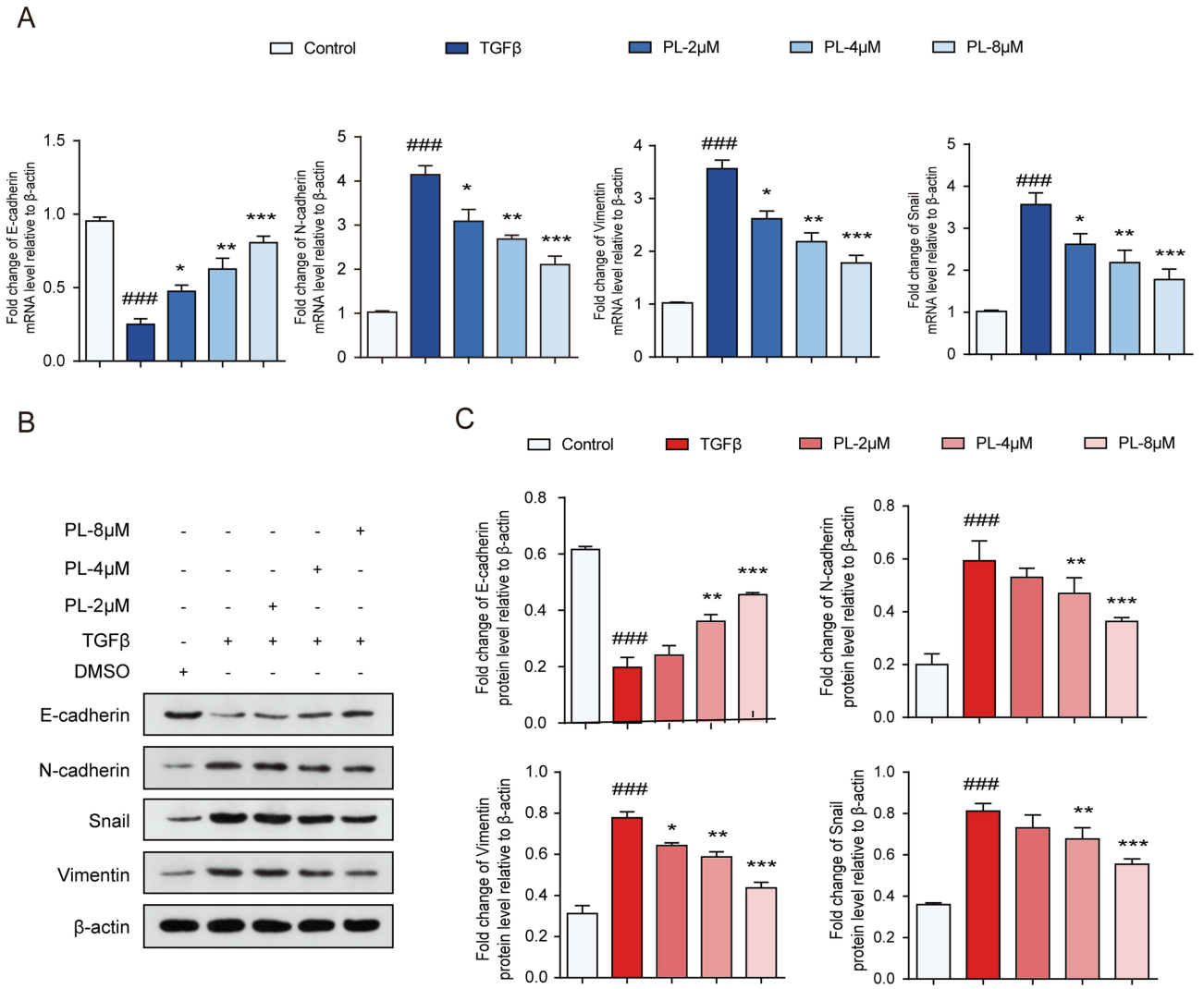

Figure 5 (**A**) mRNA levels of epithelial-mesenchymal transition (EMT) cell markers detected using quantitative polymerase chain reaction. (**B**) Protein bands corresponding to EMT cell markers detected using Western blot. (**C**) Quantitative assessment of EMT marker proteins. *$P < 0.05$, **$P < 0.01$, and ***$P < 0.001$ vs tumor growth factor-β group; ###$P < 0.001$ vs the control group.

HCC morbidity and mortality. Chinese herbal medicines and their bioactive constituents such as alkaloids, saponins, polysaccharides, flavonoids, and quinones have gained attention for their diverse pharmacological properties and demonstrated efficacy against HCC.[45–47]

The drug PL, derived from the Chinese herbal medicine Baihua Dan, has been validated for its significant anti-HCC effects. This study aimed to elucidate the anti-EMT mechanism of PL in HCC using both in vivo and in vitro experiments. PL effectively reduced HCC-associated lung metastasis in vivo. IHC and Western blot analyses of liver tissue in the in situ liver cancer model demonstrated that PL up-regulated the protein expression of E-cadherin and down-regulated that of N-cadherin, vimentin, and Snail, effectively inhibiting the EMT in HCC. In vitro, TGF-β up-regulated the expression of N-cadherin, vimentin, and Snail, while down-regulating the expression of E-cadherin at mRNA and protein levels compared to the control group. PL up-regulated the mRNA and protein expression levels of E-cadherin and decreased those of N-cadherin, vimentin, and Snail, and with the high dose of PL being the most effective. This suggests that PL can inhibit the EMT of tumor cells and thus, HCC occurrence and metastasis.

There are three types of EMT: type I occurs in embryonic development, type II occurs in tissue damage repair, and type III occurs in cancer cells, contributing to tumor initiation and progression, as well as metastasis through blood and lymphatic circulation.[48] In the transformation process of tumor cells, some epithelial cells undergo partial EMT, retaining

both epithelial and mesenchymal cell markers. These transformed epithelial cells, with the ability to migrate, may undergo mesenchymal to epithelial transformation (MET) when stimulated by the local environment in new areas. This process promotes cell proliferation and permanently immobilizes cancer cells (MET).[12,41] EMT-MET is required for metastatic colonization and plays a key role in intrahepatic and extrahepatic metastases.[49]

Pinzani proposed a more flexible interpretation of EMT-MET. In HCC development, compared to the tumor-stromal boundary, the tumor center exhibits hypoxia, inflammation, and necrosis, exhibiting a mesenchymal phenotype in response to the harsh environment, known as the "escape response"[50] Therefore, EMT transformation of HCC cells yields mesenchymal progeny with anti-apoptotic, migratory, and drug-resistant properties.[51] HCC cells acquire stem cell-like properties resembling cancer stem cells (CSC) post-EMT,[52] a factor believed to contribute to tumor recurrence and drug resistance.[53] TGF-β-stimulated HCC cells undergoing EMT are resistant to sorafenib-induced apoptosis.[54]

As mentioned above, EMT occurrence in HCC involves reprogramming epithelial gene expression, primarily activated by EMT-TF, with Snail being a critical inducer.[9,36] Additionally, an increase in hypoxia-inducible factor-1 (HIF-α) levels in breast cancer can lead to the increase of Snail expression and induce the occurrence of EMT. PL effectively down-regulated the protein levels of HIF-1α in HepG2 cells.[55] Therefore, we hypothesized that PL inhibits the EMT of HCC by regulating HIF-1α levels.

Snail, an unstable protein with a very short half-life, is a widely recognized inhibitor of E-cadherin expression.[56] It inhibits the expression of the epithelial marker gene CDH1, encoding E-cadherin, by directly suppressing E-cadherin transcription, thereby co-inducing EMT.[57] Additionally, Snail induces EMT by regulating the expression of cytoskeleton proteins, leading to biophysical changes associated with tumor metastasis.[58] Snail reduces the metastasis-inhibitory effect of E-cadherin by inducing the expression of E-cadherin repressors, such as Zeb-1 and Zeb-2.[59] Furthermore, Snail-induced EMT is implicated in the regulation of drug/immune resistance and the phenotyping of CSC.[60] High Snail expression correlates with increased tumor malignancy and poor prognosis, serving as a marker for poor prognosis in liver, stomach, and bladder cancers.

Therefore, Snail emerges as an effective target to prevent tumor metastasis, while PL can effectively inhibit its expression. E-cadherin, a transmembrane glycoprotein encoded by CDH1, is the most important component of adhesion junctions, promoting epithelial cell adhesion and serving as the main organizer of the epithelial phenotype.[61] Snail-mediated downregulation of the expression of E-cadherin enables epithelial cells to acquire a mesenchymal cell phenotype, facilitating cell migration, invasion, and metastasis.[62] Promoter methylation of E-cadherin exists in various epithelial cancer cells, including gastric and liver cancers.[63] During EMT, the up-regulation of E-cadherin leads to the instability of the cadherin-catenin complex, from which β-catenin dissociates as a transcriptional activator of cell proliferation, causing cadherin switching and the dissociation of β-catenin, which functions as a transcriptional activator of cell proliferation, resulting in the upregulation of N-cadherin.[64] When this occurs, the cadherin-catenin complex fails to bind to the actin cytoskeleton, resulting in impaired cell adhesion and enhanced motor ability.[65] N-cadherin activates the ErbB pathway by up-regulating growth factor receptor binding protein 2 (GRB2), SHC-transforming protein, and extracellular signal-regulated kinase (ERK) levels, thereby inducing EMT and tumor stem-like features. N-cadherin regulates vimentin transcription through the MAPK/ERK and phosphoinositide 3-kinase/protein kinase B signal transduction pathways, promoting EMT occurrence and HCC-associated metastasis.[66]

Vimentin, a 57 kD intermediate filament protein widely expressed in mesenchymal cells, serves as a marker of epithelial cells.[67] The expression level of vimentin is positively correlated with the invasion and metastatic ability of HCC cells.[68] Vimentin plays a multifaceted role in tumor initiation, EMT, and metastatic dissemination of tumor cells. It is an important component in the regulation of EMT, contributing to major signaling pathways in EMT, tumor progression, cell migration, invasion, and organelle localization and anchoring. Vimentin influences cell adhesion, both intercellular and with the extracellular matrix, making it an important regulator of cell movement.[69] Additionally, it promotes cell invasion by regulating the E-cadherin/β-catenin complex, exerting a more critical impact on the metastatic process than the complex itself.[70]

PL was shown to significantly inhibit HCC by impeding EMT. In previous studies, PL inhibited HCC tumor angiogenesis, invasion, and metastasis, and induced autophagy-apoptosis interaction. These findings position PL as a promising anti-HCC drug, with higher concentrations correlating with enhanced anti-HCC efficacy. However, due to poor

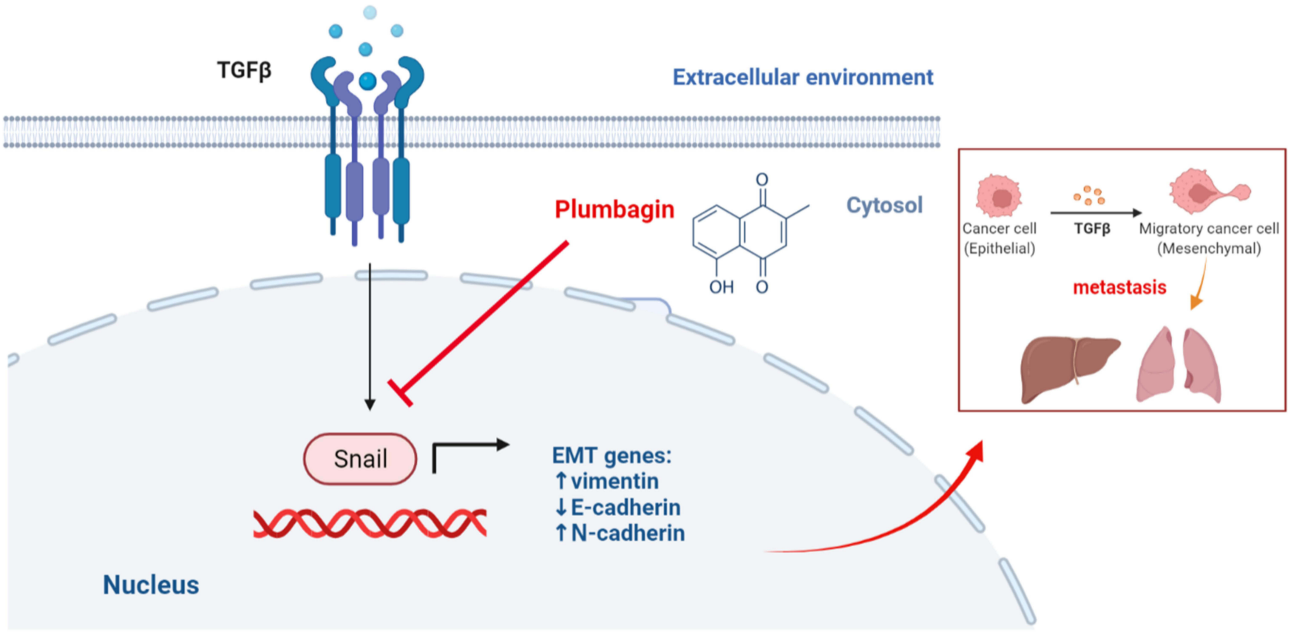

Figure 6 Mechanism of plumbagin-induced Snail and hepatocellular carcinoma epithelial-mesenchymal transition inhibition.

water solubility and biocompatibility coupled with a short retention time and fluctuating blood concentrations, the use of PL necessitates careful consideration of dosage. Thus, the effective anti-cancer dose cannot be reached, and the therapeutic effect cannot be achieved.[71] To optimize PL's anti-HCC effects, the development of suitable carriers, dosage forms, and administration methods is essential.[72] Nanocarriers, a current research focus, offer the potential to enhance the advantages of drugs while mitigating adverse reactions, maintaining steady blood concentrations, and improving solubility.[73] Current research explores nanotherapy for HCC by utilizing nanostructures to deliver traditional drug molecules. Thus, curcumin inhibits EMT and metastasis in HCC cells by down-regulating the Wnt/β-catenin signaling pathway.[74] Utilizing mesoporous silica nanostructures as carriers for curcumin, enables continuous drug release, exerting tumor toxicity and inhibiting HCC progression while enhancing bioavailability.[75,76] Loading curcumin and resveratrol onto nanostructures, particularly those surface-modified with SP94 peptide, enhances the targeting of HCC cells. Capitalizing on the enhanced permeability and retention effect, these nanostructures accumulate at the tumor site, significantly boosting the anti-metastatic and anti-EMT effects of the active substances against HCC. They release the drug in a prolonged manner and enhance the bioavailability of the drug.[77] Moreover, when organic compound molecules extracted from traditional Chinese medicine are combined with first-line antitumor drugs, the use of nanoparticle carriers can avoid the shortcomings of high side effects and poor pharmacokinetics, showing excellent antitumor efficacy and safety.[78] Despite the practicality of nanoparticles as drug carriers, challenges such as long-term stability and safety persist.[79] Therefore, identifying reasonable, effective, and safe nanostructures to deliver anti-HCC molecules, including PL, represents a future research direction.

Conclusions

In response to harsh environmental conditions such as hypoxia and inflammation, HCC initiates the EMT, increasing Snail expression, inhibiting the expression of E-cadherin, up-regulating N-cadherin, and inducing vimentin transcription through modulation of specific signaling pathways. This results in epithelial cells acquiring a mesenchymal phenotype, promoting EMT and HCC-associated metastasis. PL can prevent the EMT in HCC cells by inhibiting Snail expression and reducing lung metastasis (Figure 6). Consistent with previous studies, PL is a potential anti-therapeutic agent for HCC, with its anti-HCC efficacy increasing with the dosage increase. Further research is needed to support the clinical use of PL in the treatment of HCC. Future research trends should focus on the exploration of PL combined with first-line HCC drugs (such as TKI, ICI, capecitabine) to provide guidance for clinical treatment. Additionally, further exploration

of nanoparticle-related HCC therapy is warranted, allowing the use of green synthetic nanostructures for PL delivery in HCC treatment.

Acknowledgments

The authors gratefully acknowledge the participants who volunteered to help with the present study.

Funding

The authors gratefully acknowledge financial support by the National Natural Science Foundation of China (No. 81760757), the Key projects of Guangxi Natural Science Foundation (2019JJD140032/2019GXNSFDA245003), the second batch of"Qihuang Project" high-level talent team cultivation project of Guangxi University of Traditional Chinese Medicine (2021001).

Disclosure

The authors report no conflicts of interest in this work.

References

1. Sung H, Ferlay J, Siegel RL, et al. Global Cancer Statistics 2020: GLOBOCAN Estimates of Incidence and Mortality Worldwide for 36 Cancers in 185 Countries. *CA Cancer J Clin*. 2021;71(3):209–249. doi:10.3322/caac.21660
2. European Association for Study of Liver; European Organisation for Research and Treatment of Cancer. EASL-EORTC clinical practice guidelines: management of hepatocellular carcinoma [published correction appears in Eur J Cancer. 2012 May;48(8):1255-6]. *Eur J Cancer*. 2012;48(5):599–641. doi:10.1016/j.ejca.2011.12.021
3. McGlynn KA, Petrick JL, El-Serag HB. Epidemiology of Hepatocellular Carcinoma. *Hepatology*. 2021;73(Suppl 1):4–13. doi:10.1002/hep.31288
4. Vogel A, Meyer T, Sapisochin G, Salem R, Saborowski A. Hepatocellular carcinoma. *Lancet*. 2022;400(10360):1345–1362. doi:10.1016/S0140-6736(22)01200-4
5. Wang X, Yu GY, Chen M, Wei R, Chen J, Wang Z. Pattern of distant metastases in primary extrahepatic bile-duct cancer: a SEER-based study. *Cancer Med*. 2018;7(10):5006–5014. doi:10.1002/cam4.1772
6. Thiery JP, Acloque H, Huang RY, Nieto MA. Epithelial-mesenchymal transitions in development and disease. *Cell*. 2009;139(5):871–890. doi:10.1016/j.cell.2009.11.007
7. Navas T, Kinders RJ, Lawrence SM, et al. Clinical evolution of epithelial-mesenchymal transition in human carcinomas. *Cancer Res*. 2020;80(2):304–318. doi:10.1158/0008-5472.CAN-18-3539
8. Brabletz T, Kalluri R, Nieto MA, Weinberg RA. EMT in cancer. *Nat Rev Cancer*. 2018;18(2):128–134. doi:10.1038/nrc.2017.118
9. Brabletz S, Schuhwerk H, Brabletz T, Stemmler MP. Dynamic EMT: a multi-tool for tumor progression. *EMBO J*. 2021;40(18):e108647. doi:10.15252/embj.2021108647
10. Song S, Qiu X. LncRNA miR503HG inhibits epithelial-mesenchymal transition and angiogenesis in hepatocellular carcinoma by enhancing PDCD4 via regulation of miR-15b [published correction appears in Dig Liver Dis. 2021 Jul 9]. *Dig Liver Dis*. 2021;53(1):107–116. doi:10.1016/j.dld.2020.09.008
11. Xiao S, Hu J, Hu N, Sheng L, Rao H, Zheng G. Identification of a novel epithelial-to-mesenchymal-related gene signature in predicting survival of patients with hepatocellular carcinoma. *Comb Chem High Throughput Screen*. 2022;25(8):1254–1270. doi:10.2174/1386207324666210303093629
12. Pei D, Shu X, Gassama-Diagne A, Thiery JP. Mesenchymal-epithelial transition in development and reprogramming. *Nat Cell Biol*. 2019;21(1):44–53. doi:10.1038/s41556-018-0195-z
13. Xia P, Zhang H, Xu K, et al. MYC-targeted WDR4 promotes proliferation, metastasis, and sorafenib resistance by inducing CCNB1 translation in hepatocellular carcinoma. *Cell Death Dis*. 2021;12(7):691. doi:10.1038/s41419-021-03973-5
14. Fischer KR, Durrans A, Lee S, et al. Epithelial-to-mesenchymal transition is not required for lung metastasis but contributes to chemoresistance. *Nature*. 2015;527(7579):472–476. doi:10.1038/nature15748
15. Zheng X, Carstens JL, Kim J, et al. Epithelial-to-mesenchymal transition is dispensable for metastasis but induces chemoresistance in pancreatic cancer. *Nature*. 2015;527(7579):525–530. doi:10.1038/nature16064
16. Galle E, Thienpont B, Cappuyns S, et al. DNA methylation-driven EMT is a common mechanism of resistance to various therapeutic agents in cancer. *Clin Epigenet*. 2020;12(1):27. doi:10.1186/s13148-020-0821-z
17. Li Z, Zhang Z, Fang L, et al. Tumor microenvironment composition and related therapy in hepatocellular carcinoma. *J Hepatocell Carcinoma*. 2023;10:2083–2099. doi:10.2147/JHC.S436962
18. Xutian S, Cao D, Wozniak J, Junion J, Boisvert J. Comprehension of the unique characteristics of traditional Chinese medicine. *Am J Chin Med*. 2012;40(2):231–244. doi:10.1142/S0192415X12500188
19. Kong D, Zhang F, Shao J, et al. Curcumin inhibits cobalt chloride-induced epithelial-to-mesenchymal transition associated with interference with TGF-β/Smad signaling in hepatocytes. *Lab Invest*. 2015;95(11):1234–1245. doi:10.1038/labinvest.2015.107
20. Iqbal J, Abbasi BA, Batool R, et al. Potential phytocompounds for developing breast cancer therapeutics: nature's healing touch. *Eur J Pharmacol*. 2018;827:125–148. doi:10.1016/j.ejphar.2018.03.007
21. Ijaz S, Akhtar N, Khan MS, et al. Plant derived anticancer agents: a green approach towards skin cancers. *Biomed Pharmacother*. 2018;103:1643–1651. doi:10.1016/j.biopha.2018.04.113
22. Tripathi SK, Panda M, Biswal BK. Emerging role of plumbagin: cytotoxic potential and pharmaceutical relevance towards cancer therapy. *Food Chem Toxicol*. 2019;125:566–582. doi:10.1016/j.fct.2019.01.018

23. Yu T, Xu YY, Zhang YY, Li KY, Shao Y, Liu G. Plumbagin suppresses the human large cell lung cancer cell lines by inhibiting IL-6/STAT3 signaling in vitro. *Int Immunopharmacol*. 2018;55:290–296. doi:10.1016/j.intimp.2017.12.021
24. Pradubyat N, Sakunrangsit N, Mutirangura A, Ketchart W. NADPH: quinone oxidoreductase 1 (NQO1) mediated anti-cancer effects of plumbagin in endocrine resistant MCF7 breast cancer cells. *Phytomedicine*. 2020;66:153133. doi:10.1016/j.phymed.2019.153133
25. Hafeez BB, Zhong W, Mustafa A, Fischer JW, Witkowsky O, Verma AK. Plumbagin inhibits prostate cancer development in TRAMP mice via targeting PKCε, Stat3 and neuroendocrine markers. *Carcinogenesis*. 2012;33(12):2586–2592. doi:10.1093/carcin/bgs291
26. Sakunrangsit N, Ketchart W. Plumbagin inhibits cancer stem-like cells, angiogenesis and suppresses cell proliferation and invasion by targeting Wnt/β-catenin pathway in endocrine resistant breast cancer. *Pharmacol Res*. 2019;150:104517. doi:10.1016/j.phrs.2019.104517
27. Lin Y, Chen Y, Wang S, et al. Plumbagin induces autophagy and apoptosis of SMMC-7721 cells in vitro and in vivo. *J Cell Biochem*. 2019;120 (6):9820–9830. doi:10.1002/jcb.28262
28. Wei Y, Lv B, Xie J, et al. Plumbagin promotes human hepatoma SMMC-7721 cell apoptosis via caspase-3/vimentin signal-mediated EMT. *Drug Des Devel Ther*. 2019;13:2343–2355. doi:10.2147/DDDT.S204787
29. Wei Y, Yang Q, Zhang Y, et al. Plumbagin restrains hepatocellular carcinoma angiogenesis by suppressing the migration and invasion of tumor-derived vascular endothelial cells. *Oncotarget*. 2017;8(9):15230–15241. doi:10.18632/oncotarget.14774
30. Zhong J, Li J, Wei J, et al. Plumbagin restrains hepatocellular carcinoma angiogenesis by stromal cell-derived factor (SDF-1)/CXCR4-CXCR7 axis. *Med Sci Monit*. 2019;25:6110–6119. doi:10.12659/MSM.915782
31. Liu H, Zhang W, Jin L, Liu S, Liang L, Wei Y. Plumbagin exhibits genotoxicity and induces G2/M cell cycle arrest via ros-mediated oxidative stress and activation of ATM-p53 signaling pathway in hepatocellular cells. *Int J Mol Sci*. 2023;24(7):6279. doi:10.3390/ijms24076279
32. Zhou R, Wu K, Su M, Li R. Bioinformatic and experimental data decipher the pharmacological targets and mechanisms of plumbagin against hepatocellular carcinoma. *Environ Toxicol Pharmacol*. 2019;70:103200. doi:10.1016/j.etap.2019.103200
33. Li CM, Zhang J, Wu W, et al. FBXO43 increases CCND1 stability to promote hepatocellular carcinoma cell proliferation and migration. *Front Oncol*. 2023;13:1138348. doi:10.3389/fonc.2023.1138348
34. Zhang B, Li F, Zhu Z, Ding A, Luo J. CircRNA CDR1as/miR-1287/Raf1 axis modulates hepatocellular carcinoma progression through MEK/ERK pathway. *Cancer Manag Res*. 2020;12:8951–8964. doi:10.2147/CMAR.S252679
35. Ye Y, Guo J, Xiao P, et al. Macrophages-induced long noncoding RNA H19 up-regulation triggers and activates the miR-193b/MAPK1 axis and promotes cell aggressiveness in hepatocellular carcinoma. *Cancer Lett*. 2020;469:310–322. doi:10.1016/j.canlet.2019.11.001
36. Kong F, Ma L, Wang X, You H, Zheng K, Tang R. Regulation of epithelial-mesenchymal transition by protein lysine acetylation. *Cell Commun Signal*. 2022;20(1):57. doi:10.1186/s12964-022-00870-y
37. van Zijl F, Krupitza G, Mikulits W. Initial steps of metastasis: cell invasion and endothelial transmigration. *Mutat Res*. 2011;728(1–2):23–34. doi:10.1016/j.mrrev.2011.05.002
38. Bruix J, Gores GJ, Mazzaferro V. Hepatocellular carcinoma: clinical frontiers and perspectives. *Gut*. 2014;63(5):844–855. doi:10.1136/gutjnl-2013-306627
39. Liu CY, Chen KF, Chen PJ. Treatment of Liver Cancer. *Cold Spring Harb Perspect Med*. 2015;5(9):a021535. doi:10.1101/cshperspect.a021535
40. Zou J, Li H, Huang Q, et al. Dopamine-induced SULT1A3/4 promotes EMT and cancer stemness in hepatocellular carcinoma. *Tumour Biol*. 2017;39(10):1010428317719272. doi:10.1177/1010428317719272
41. Giannelli G, Koudelkova P, Dituri F, Mikulits W. Role of epithelial to mesenchymal transition in hepatocellular carcinoma. *J Hepatol*. 2016;65 (4):798–808. doi:10.1016/j.jhep.2016.05.007
42. Trevisani F, Brandi G, Garuti F, et al. Metronomic capecitabine as second-line treatment for hepatocellular carcinoma after sorafenib discontinuation. *J Cancer Res Clin Oncol*. 2018;144(2):403–414. doi:10.1007/s00432-017-2556-6
43. Khanam A, Kottilil S. New Therapeutics for HCC: does Tumor immune microenvironment matter? *Int J Mol Sci*. 2022;24(1):437. doi:10.3390/ijms24010437
44. Stefanini B, Ielasi L, Chen R, et al. TKIs in combination with immunotherapy for hepatocellular carcinoma. *Expert Rev Anticancer Ther*. 2023;23 (3):279–291. doi:10.1080/14737140.2023.2181162
45. Liu X, Li M, Wang X, et al. Effects of adjuvant traditional Chinese medicine therapy on long-term survival in patients with hepatocellular carcinoma. *Phytomedicine*. 2019;62:152930. doi:10.1016/j.phymed.2019.152930
46. Park J, Jeong D, Song M, Kim B. Recent advances in anti-metastatic approaches of herbal medicines in 5 major cancers: from traditional medicine to modern drug discovery. *Antioxidants*. 2021;10(4):527. doi:10.3390/antiox10040527
47. Li JJ, Liang Q, Sun GC. Traditional Chinese medicine for prevention and treatment of hepatocellular carcinoma: a focus on epithelial-mesenchymal transition. *J Integr Med*. 2021;19(6):469–477. doi:10.1016/j.joim.2021.08.004
48. Lamouille S, Xu J, Derynck R. Molecular mechanisms of epithelial-mesenchymal transition. *Nat Rev Mol Cell Biol*. 2014;15(3):178–196. doi:10.1038/nrm3758
49. Nieto MA. Epithelial plasticity: a common theme in embryonic and cancer cells. *Science*. 2013;342(6159):1234850. doi:10.1126/science.1234850
50. Pinzani M. Epithelial-mesenchymal transition in chronic liver disease: fibrogenesis or escape from death? *J Hepatol*. 2011;55(2):459–465. doi:10.1016/j.jhep.2011.02.001
51. Jou J, Diehl AM. Epithelial-mesenchymal transitions and hepatocarcinogenesis. *J Clin Invest*. 2010;120(4):1031–1034. doi:10.1172/JCI42615
52. Liang L, Kaufmann AM. The significance of cancer stem cells and epithelial-mesenchymal transition in metastasis and anti-cancer therapy. *Int J Mol Sci*. 2023;24(3):2555. doi:10.3390/ijms24032555
53. Seebacher NA, Krchniakova M, Stacy AE, Skoda J, Jansson PJ. Tumour microenvironment stress promotes the development of drug resistance. *Antioxidants*. 2021;10(11):1801. doi:10.3390/antiox10111801
54. Fernando J, Malfettone A, Cepeda EB, et al. A mesenchymal-like phenotype and expression of CD44 predict lack of apoptotic response to sorafenib in liver tumor cells. *Int, J, Cancer*. 2015;136(4):E161–E172. doi:10.1002/ijc.29097
55. Yanfei W, Beibei L, Lijie J, et al. Effects of Leucodanone on proliferation, apoptosis, invasion and HIF-1α expression of hepatocellular carcinoma HepG2 cells under hypoxia. *Chin Modern Appl Pharm*. 2022;33(14):1789–1795.
56. Alba-Castellón L, Olivera-Salguero R, Mestre-Farrera A, et al. Snail1-dependent activation of cancer-associated fibroblast controls epithelial tumor cell invasion and metastasis. *Cancer Res*. 2016;76(21):6205–6217. doi:10.1158/0008-5472.CAN-16-0176

57. Long X, Wang DG, Wu ZB, Liao ZM, Xu JJ. Circular RNA hsa_circ_0004689 (circSWT1) promotes NSCLC progression via the miR-370-3p/SNAIL axis by inducing cell epithelial-mesenchymal transition (EMT). *Cancer Med*. 2023;12(7):8289–8305. doi:10.1002/cam4.5527
58. Hu Y, Li Q, Yi K, et al. HuR affects the radiosensitivity of esophageal cancer by regulating the EMT-related protein snail. *Front Oncol*. 2022;12:883444. doi:10.3389/fonc.2022.883444
59. Smith BN, Odero-Marah VA. The role of Snail in prostate cancer. *Cell Adh Migr*. 2012;6(5):433–441. doi:10.4161/cam.21687
60. Wang W, Liu W, Chen Q, Yuan Y, Wang P. Targeting CSC-related transcription factors by E3 ubiquitin ligases for cancer therapy. *Semin Cancer Biol*. 2022;87:84–97. doi:10.1016/j.semcancer.2022.11.002
61. Tian Y, Qi P, Niu Q, Hu X. Combined snail and E-cadherin predicts overall survival of cervical carcinoma patients: comparison among various epithelial-mesenchymal transition proteins. *Front Mol Biosci*. 2020;7:22. doi:10.3389/fmolb.2020.00022
62. Steinbichler TB, Dudas J, Ingruber J, et al. Slug is a surrogate marker of Epithelial to Mesenchymal Transition (EMT) in head and neck cancer. *J Clin Med*. 2020;9(7):2061. doi:10.3390/jcm9072061
63. Maria de França G, Andrade ACM, Felix FA, et al. Survival-related epithelial-mesenchymal transition proteins in oropharyngeal squamous cell carcinoma: a systematic review and meta-analysis. *Arch Oral Biol*. 2021;131:105267. doi:10.1016/j.archoralbio.2021.105267
64. Wei J, Wu L, Yang S, et al. E-cadherin to N-cadherin switching in the TGF-β1 mediated retinal pigment epithelial to mesenchymal transition. *Exp Eye Res*. 2022;220:109085. doi:10.1016/j.exer.2022.109085
65. Pettitt J. The cadherin superfamily. *WormBook*. 2005;1–9. doi:10.1895/wormbook.1.50.1
66. Liu PF, Kang BH, Wu YM, et al. Vimentin is a potential prognostic factor for tongue squamous cell carcinoma among five epithelial-mesenchymal transition-related proteins. *PLoS One*. 2017;12(6):e0178581. doi:10.1371/journal.pone.0178581
67. Liu CY, Lin HH, Tang MJ, Wang YK. Vimentin contributes to epithelial-mesenchymal transition cancer cell mechanics by mediating cytoskeletal organization and focal adhesion maturation. *Oncotarget*. 2015;6(18):15966–15983. doi:10.18632/oncotarget.3862
68. You H, Yuan D, Bi Y, et al. Hepatitis B virus X protein promotes vimentin expression via LIM and SH3 domain protein 1 to facilitate epithelial-mesenchymal transition and hepatocarcinogenesis. *Cell Commun Signal*. 2021;19(1):33. doi:10.1186/s12964-021-00714-1
69. Kidd ME, Shumaker DK, Ridge KM. The role of vimentin intermediate filaments in the progression of lung cancer. *Am J Respir Cell Mol Biol*. 2014;50(1):1–6. doi:10.1165/rcmb.2013-0314TR
70. Xu J, Liu D, Niu H, et al. Resveratrol reverses Doxorubicin resistance by inhibiting epithelial-mesenchymal transition (EMT) through modulating PTEN/Akt signaling pathway in gastric cancer [published correction appears in J Exp Clin Cancer Res. 2023 Jan 17;42(1):23]. *J Exp Clin Cancer Res*. 2017;36(1):19. doi:10.1186/s13046-016-0487-8
71. Singh S, Sharma N, Shukla S, et al. Understanding the potential role of nanotechnology in liver fibrosis: a paradigm in therapeutics. *Molecules*. 2023;28(6):2811. doi:10.3390/molecules28062811
72. Nong J, Glassman PM, Muzykantov VR. Targeting vascular inflammation through emerging methods and drug carriers. *Adv Drug Deliv Rev*. 2022;184:114180. doi:10.1016/j.addr.2022.114180
73. Mathi Maran S. Bioengineering of nano drug delivery compound to enhance the bioavailability of selected bioactive compound. *JABB*. 2021;8(3):93–97. doi:10.15406/jabb.2021.08.00259
74. Zhu J, Qu J, Fan Y, Zhang R, Wang X. Curcumin inhibits invasion and epithelial-mesenchymal transition in hepatocellular carcinoma cells by regulating TET1/Wnt/β-catenin signal axis. *Bull Exp Biol Med*. 2022;173(6):770–774. doi:10.1007/s10517-022-05629-6
75. Kong ZL, Kuo HP, Johnson A, Wu LC, Chang KLB. Curcumin-loaded mesoporous silica nanoparticles markedly enhanced cytotoxicity in hepatocellular carcinoma cells. *Int J Mol Sci*. 2019;20(12):2918. doi:10.3390/ijms20122918
76. Wang W, Liu Q, Liang X, Kang Q, Wang Z. Protective role of naringin loaded solid nanoparticles against aflatoxin B1 induced hepatocellular carcinoma. *Chem Biol Interact*. 2022;351:109711. doi:10.1016/j.cbi.2021.109711
77. Zheng Y, Jia R, Li J, Tian X, Qian Y. Curcumin- and resveratrol-co-loaded nanoparticles in synergistic treatment of hepatocellular carcinoma. *J Nanobiotechnology*. 2022;20(1):339. doi:10.1186/s12951-022-01554-y
78. Markovsky E, Baabur-Cohen H, Satchi-Fainaro R. Anticancer polymeric nanomedicine bearing synergistic drug combination is superior to a mixture of individually-conjugated drugs. *J Control Release*. 2014;187:145–157. doi:10.1016/j.jconrel.2014.05.025
79. Wang T, Zhang D, Sun D, Gu J. Current status of in vivo bioanalysis of nano drug delivery systems. *J Pharm Anal*. 2020;10(3):221–232. doi:10.1016/j.jpha.2020.05.002